Supporting Information for: "Rheological Link Between Polymer Melts with a High Molecular Weight Tail and Enhanced Formation of Shish-Kebabs"

Sara Lindeblad Wingstrand,[†] Bo Shen,[‡] Julie A. Kornfield,[‡] Kell Mortensen,[¶] Daniele Parisi,[§,‖] Dimitris Vlassopoulos,[§,‖] and Ole Hassager*[,†]

†*Technical University of Denmark, Department of Chemical and Biochemcial Engineering, Danish Polymer Center,DK-2800 Kgs. Lyngby, Denmark*

‡*California Institute of Technology, Division of Chemistry and Chemical Engineering, Pasadena, CA 91125, USA*

¶*University of Copenhagen, Niels Bohr Institute, X-ray and Neutron Science, DK-2100 København Ø, Denmark*

§*Institute of Electronic Structure and Laser, FORTH, Heraklion 71110, Crete Greece*

‖*Department of Materials Science & Technology, University of Crete, Heraklion 71003, Crete Greece*

E-mail: oh@kt.dtu.dk

Supplemental Text

Details on Rheological measurements

Creep The samples were shaped into discotic specimens at 150C using a home-made vacuum press mold for twenty minutes and then loaded on the rheometer at the same temperature. We used a stress-controlled rheometer MCR702 (Anton Paar, Austria). The specimen was placed between two stainless steel parallel plates of 8 mm diameter and gap about 0.7 mm, calibrated for thermal expansion. Temperature control was achieved by means of a hybrid temperature control system CTD180 which has intermediate characteristics between a Peltier cell and a convection oven. All tests were performed in nitrogen atmosphere in order to reduce the risk of sample degradation. The measurement protocol consisted of three steps: (i) equilibration and stability of the samples was monitored by running dynamic frequency sweep tests (SAOS) in strain-controlled mode at the same conditions and different times (starting from 20 min after loading, up to 1 hour), checking for the overlap of the dynamic moduli ; (ii) dynamic strain sweeps at 100 rad/s and varying strain amplitude from 0.1% to 10% in order to detect the limits of linear viscoelastic response; a strain amplitude of 1% was found appropriate for all tests ; (iii) dynamic frequency sweeps in the range from 100 to 0.1 rad/s in order to probe the linear viscoelastic response. Subsequently, creep experiments were performed over a range of stresses between 30 and 80 Pa. For each specimen, a creep test was repeated three times at different stresses to ensure that the measurements were performed in the linear regime (see Figure 4S. This was crucial since the creep data were eventually transformed into frequency spectra.

Filament stretching For the rheological characterization we used samples in the form of thin discs (8 mm diameter and 0.8-2 mm in height). The discs were prepared utilizing vacuum moulding at 175 °C for 25 min to ensure proper erasing of any thermo-mechanical history. We performed nonlinear extensional rheology using an FSR - Filament Stretch Rheometer (VADER 1000 from Rheofilament). The basic working principle of the instrument

is the following: A molten sample-disc sandwiched between a bottom and a top plate is deformed by moving the upper plate axially. The deformation of the sample midplane is monitored via a laser micrometer. A feedback loop enables the deformation to be controlled while the response of the material is monitored by a force cell mounted on the bottom plate. The deformation of the midfilament plane is measured in terms of Hencky strain ($\varepsilon = -2\ln\frac{D(t)}{D_0}$). Here $D(t)$ and D_0 are the diameter measured at a given time (t) and the initial diameter, respectively. The response of the material is given by the normal stress difference $\langle\sigma_{zz} - \sigma_{rr}\rangle = (F - \frac{1}{2}mg)/\frac{\pi}{4}D(t)^2$. Here F is the force measured on the bottom plate, m is the mass of the sample and g is the gravitational acceleration.

The VADER 1000 has two features that are crucial for this study. 1) The feedback control loop providing active control of the deformation and thus enables high Hencky strains ($\varepsilon > 7$) to be reached without experiencing failure due to uncontrolled neck propagation. 2) Fast oven removal enabling quench of filaments to room temperature. The oven surrounding the sample can be pushed up leaving the sample exposed to ambient conditions. The quenching rate for filaments with a diameter of 1 mm has been estimated to be $> 10\,\mathrm{K/s}$.

The experimental protocol for filament stretching was the following. The sample was pre-stretched at 150 °C and subsequently relaxed for 15 min to erase all thermo-mechanical history. We found 150 °C sufficiently high as samples relaxed at higher temperatures showed the same extensional behavior. The temperature was subsequently lowered to 140 °C, stretched at a constant Hencky strain rate $\dot{\varepsilon}$ and quenched at $\varepsilon = 5.5$. We observed no signs of flow induced crystallization during stretching. In order for all samples to experience the same quench history, the final filament diameter at quench for all samples was $0.47 - 0.5$. Ex-sity SAXS patterns of the quenched filaments were collected using a SAXSLAB instrument (Ganesha from SAXSLAB, Denmark) with a 300k Pilatus detector (pixel sizes $172\times172\mu$m). The wavelength of the X-ray beam was 1.54 Åand the sample-to-detector distance was 1491 mm. Patterns with exposure times of $6\cdot10^2$ - 10^4s were collected from the midfilament plane of vertically mounted filaments.

Multimode Maxwell model

The linear rheological response is model using the Multimode Maxwell model. It considers the total response of a material to be a sum of contributions from i number of modes with relaxation times τ_i and corresponding moduli g_i. The storage modulus G' and loss modulus G'' is thus given by:

$$G' = \sum_i \frac{g_i(\tau_i\omega)^2}{1+(\tau_i\omega)^2} \tag{1}$$

$$G'' = \sum_i \frac{g_i\tau_i\omega}{1+(\tau_i\omega)^2} \tag{2}$$

We used the software Reptate to perform the fit. The full Maxwell spectrum is given in Table 1S

Hermans Orientation factor from SAXS

The average cosine squared ($\langle\cos^2\phi\rangle$) of the angle between the normal of a plane in the crystalline domains and the macroscopic direction in Eq. (1) of the main article, can be determined from azimuthally integrated SAXS patterns using:

$$\left\langle\cos^2\phi\right\rangle = \frac{\int_0^{\pi/2} I_\beta \cos^2\beta \sin\beta \,\mathrm{d}\,\beta}{\int_0^{\pi/2} I_\beta \sin\beta \,\mathrm{d}\,\beta} \tag{3}$$

Here β is the azimuthal angle and I_β is the corresponding intensity corrected for the contribution from shish.

The SAXS patterns obtained in this work show a significant scattering contribution from shish (see intensity peak along the equatorial in Figure 1S (a). The resulting azimuthal intensity profiles from which F_H is extracted thus contains unwanted peaks at $\pi/2$ and $3\pi/2$ that does not arise from kebab-scattering. (see Figure1S (b). This contribution must be subtracted to obtain the correct values of F_H. The shish contribution is subtracted from

the azimuthal intensity profiles by decomposition into an intensity contribution from kebabs (I_k) and shish (I_s) as well as an isotropic contribution I_{iso}.

$$I = I_k + I_s + I_{iso} \tag{4}$$

The two peak contributions I_k and I_s are described by periodically spaced peaks with a Lorentzian type distribution, while I_{iso} is a constant:

$$I_{kebab} = \frac{I_k}{1 + \left(\frac{\beta - (p\pi + \beta_0)}{\gamma_k}\right)^2} \qquad I_{shish} = \frac{I_s}{1 + \left(\frac{\beta - (\pi(p+1/2) + \beta_0)}{\gamma_s}\right)^2} \qquad I_{iso} = const. \tag{5}$$

Here I_k and I_s are the maximum intensities of the kebab and shish peaks, repspectively while γ_k and γ_s are the corresponding "half width at half maxmimum" of the peaks. β_0 enables a horizontal shift for samples that where slightly rotated in the beamline during the recording of the SAXS patterns. $p = -1, 0, 1, 2$ and ensures that all periodic peaks contributing to the patterns are included. To obtain an expression for the the azimuthal intensity profile I_β without the shish contribution we simply subtract I_s from the raw data I_{raw} such that:

$$I_\beta = I_{raw} - I_s \tag{6}$$

From this it is now possible to obtain a more accurate value of F_H

Supporting Tables

Table 1S: Multimode Maxwell parameters for the UH-blend and the matrix at $T = 140°C$

	UH-blend		**Matrix**	
mode, i	$\boldsymbol{\tau_i}$ **[s]**	$\mathbf{g_i}$ [Pa]	$\boldsymbol{\tau_i}$ **[s]**	$\mathbf{g_i}$ [Pa]
10	1.4E+03	2.4E+01	1.3E+03	1.1E-02
9	3.1E+02	1.8E+01	3.0E+02	1.7E+01
8	7.0E+01	1.5E+02	6.9E+01	6.0E+01
7	1.6E+01	5.5E+02	1.6E+01	3.8E+02
6	3.5E+00	2.4E+03	3.5E+00	2.2E+03
5	7.9E-01	1.2E+04	8.0E-01	1.1E+04
4	1.8E-01	4.4E+04	1.8E-01	4.6E+04
3	4.0E-02	1.4E+05	4.1E-02	1.4E+05
2	8.9E-03	2.3E+05	9.4E-03	2.1E+05
1	2.0E-03	5.6E+05	2.1E-03	5.4E+05

Supporting Figures

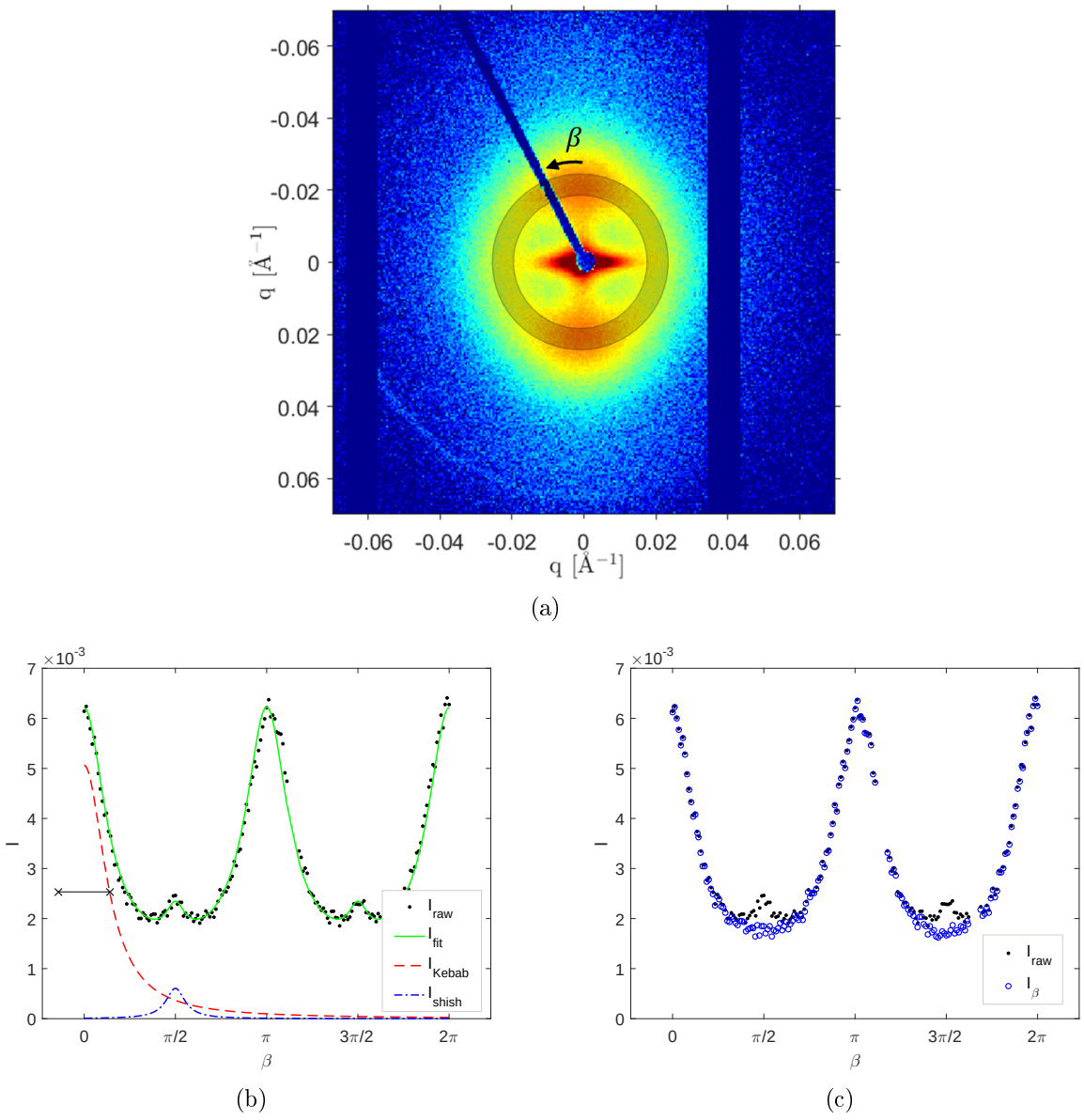

Figure 1S: Illutration of how scattering intensities from kebabs are extracted from SAXS-patterns while omitting the contribution from shish. (a) Example of the raw SAXS pattern. The shaded area indicate the area over which the azimuthal integration is performed. With the arrow showing the direction of the azimuthal angle β. (b) Azimuthal intensity profile where (black $\cdot$) is the raw data, (green $-$) is the total fit using Eq. (4) with (red $--$) and (blue $\cdot-$) signifying the scattering contribution from kebabs and shish, respectively, with $p = -1$. (c) Compares the raw azimuthal intensity profile (black $\cdot$) and the profile where the shish-contribution has been removed (blue $\circ$) by subtracting the fitted shich contribution shown in (b).

.

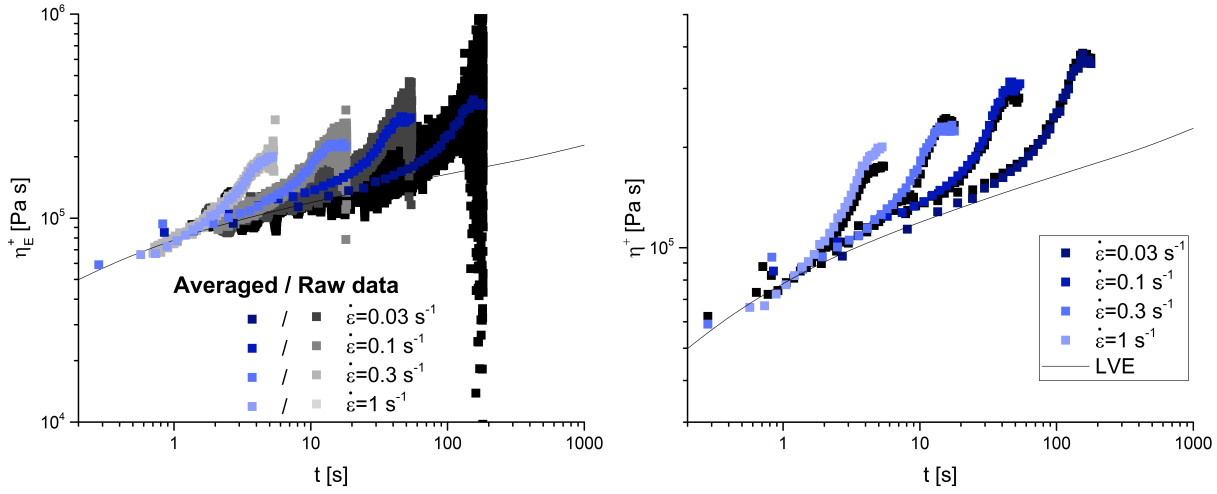

Figure 2S: Uniaxial extensional data for the UH-blend at 140°C (a) Shows the raw data (gray scale symbols) and the averaged data (blue scale symbols) (b) Shows the reproducibility of the stretches for two sets of stretch experiments (blue and black symbols, respectively)

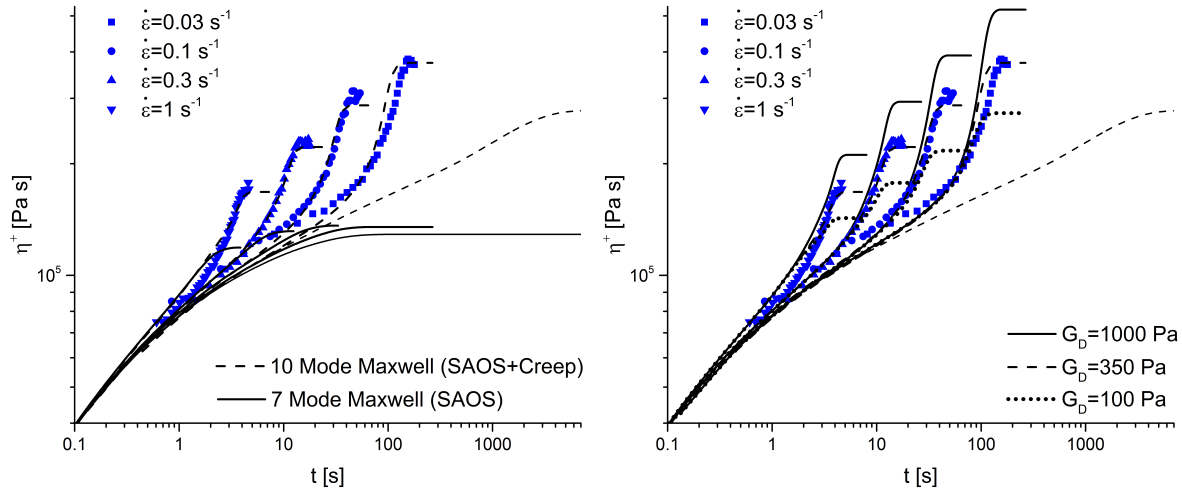

Figure 3S: Parameter Sensitivity for the HMMSF modelling (lines) of constant rate extensional data (symbols) at 140°C. (a) Compares the HMMSF prediction using the full 10 mode frequency Maxwell spectrum obtained by combining SAOS and creep data with the prediction using the limited 7 mode spectrum obtained from SAOS alone. (b) Shows the HMMSF prediction using different values of G_D.

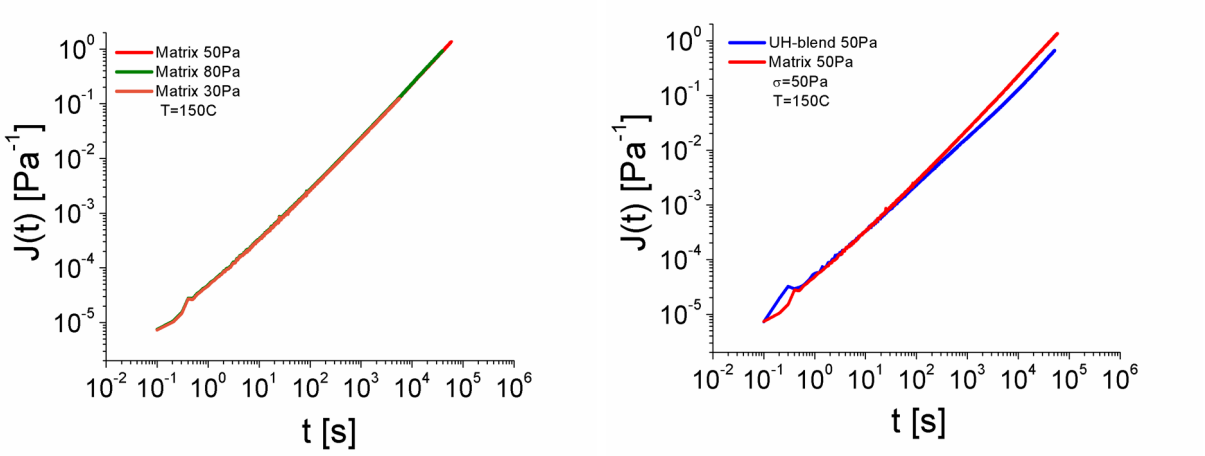

(a) (b)

Figure 4S: Rheological response in creep. (a) Creep compliance curves for the matrix obtained at various stresses at 150°C. The overlap confirms that measurements are performed in the linear regime. (b) Comparison of creep compliance curves for the UH-blend and the matrix.

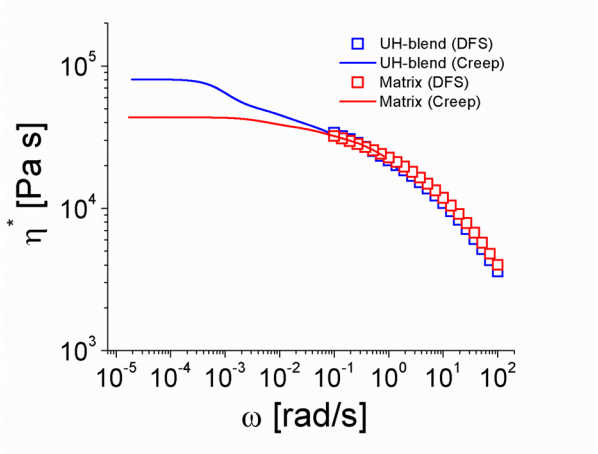

Figure 5S: Dynamic shear viscosity 150°C for the UH-blend and the matrix obtained via SAOS (symbols) and creep (lines). Note the difference in zero-shear-rate viscosity at low frequencies

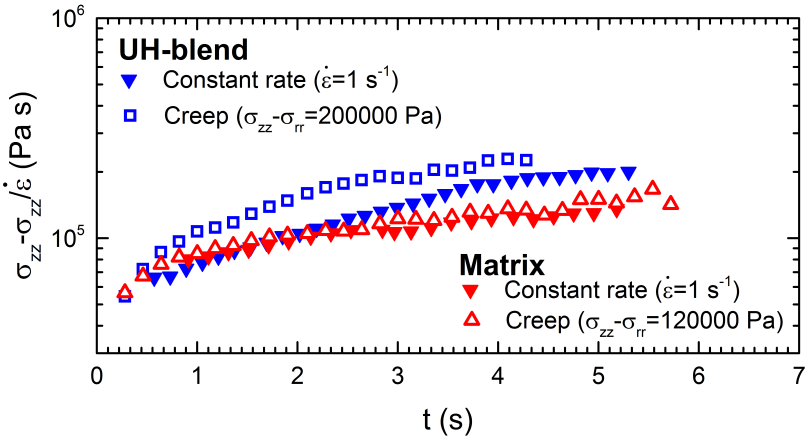

Figure 6S: Uniaxial extensional response for complementary experiments in creep (open symbols) and constant rate (closed symbols) at 140°C showing the same steady flow behavior for the UH-blend (blue) and the matrix (red).

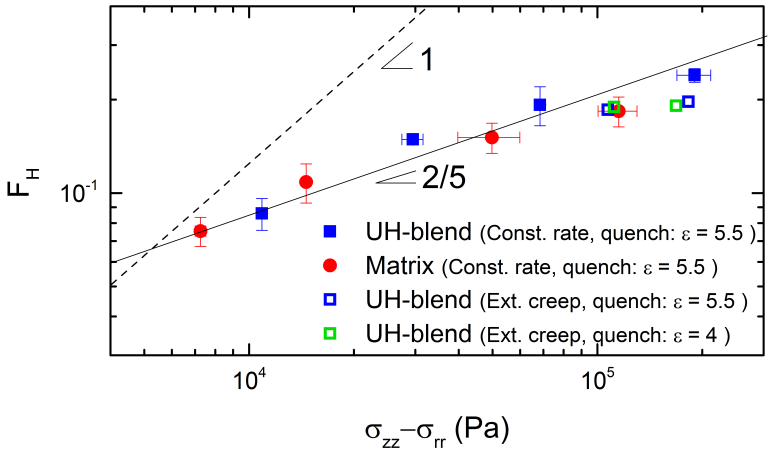

Figure 7S: Herman's orientation factor versus steady stress UH-blend (blue) and matrix (red) for filaments elongated at a constant Hencky strain rate. Black solid and dashed lines show the apparent slope of 2/5 and the expected trend for amorphous systems, respectively. Open symbols represent Herman's orientation factor for filaments of the UH-blend obtained for uniaxial creep measurements, quenched at $\varepsilon = 4$ (green) and 5.5 (blue). Apart from the open symbols, this figure is identical to Figure 5 in the main manuscript.